

## JB Review

# Harnessing biomolecular condensates in living cells

Received January 28, 2019; accepted April 22, 2019; published online April 24, 2019

**Hideki Nakamura\***, **Robert DeRose** and **Takanari Inoue†**

Department of Cell Biology and Center for Cell Dynamics, Johns Hopkins University School of Medicine, 855 N. Wolfe Street, Baltimore, MD 21205, USA

\*Hideki Nakamura, Department of Cell Biology and Center for Cell Dynamics, Johns Hopkins University School of Medicine, 855 N. Wolfe Street, Baltimore, MD 21205, USA. Tel: +1 443 287 7669, Fax: +1 443 287 8375, email: hnakamu2@jhmi.edu

†Takanari Inoue, Department of Cell Biology and Center for Cell Dynamics, Johns Hopkins University School of Medicine, 855 N. Wolfe Street, Baltimore, MD 21205, USA. email: jctinoue@jhmi.edu

**As part of the ‘Central Dogma’ of molecular biology, the function of proteins and nucleic acids within a cell is determined by their primary sequence. Recent work, however, has shown that within living cells the role of many proteins and RNA molecules can be influenced by the physical state in which the molecule is found. Within living cells, both protein and RNA molecules are observed to condense into non-membrane-bound yet distinct structures such as liquid droplets, hydrogels and insoluble aggregates. These unique intracellular organizations, collectively termed biomolecular condensates, have been found to be vital in both normal and pathological conditions. Here, we review the latest studies that have developed molecular tools attempting to recreate artificial biomolecular condensates in living cells. We will describe their design principles, implementation and unique characteristics, along with limitations. We will also introduce how these tools can be used to probe and perturb normal and pathological cell functions, which will then be complemented with discussions of remaining areas for technological advance under this exciting theme.**

**Keywords:** biomolecular condensates; liquid droplets; hydrogels; chemically-induced dimerization; optogenetics.

**Abbreviations:** ALS, amyotrophic lateral sclerosis; Fluoppi, fluorescent protein–protein–interaction–visualization; FRAP, fluorescence recovery after photobleaching; IDR, intrinsically disordered region; PPI, protein–protein interaction; PRM, proline-rich motif; RNP, ribonucleoprotein; SH3, SRC homology 3.

## Biomolecular Condensates: Re-discovered in Light of Diverse Physical States

Among diverse classes of intriguing intracellular structures, membrane-bound organelles have been the best-known and the best-studied for decades. However, the

importance of non-membrane-bound counterparts, recently known as biomolecular condensates, has been attracting more and more attentions in recent biological researches (1). They are observed in different biological contexts ranging from basic and essential physiological processes such as transcription (2, 3) and stress response (4), to severe pathophysiological situations including neurodegenerative diseases (5) (Fig. 1A, vertical axis).

Despite their involvement in such diverse functions, these condensates share many features in common, especially in terms of molecular dynamics and mechanisms of condensation (6–8). They are often associated with certain physical states such as liquid droplets, hydrogels or irreversible aggregates, according to the extent of their dynamic nature. These physical states are achieved by the constituent biomolecules undergoing phase behaviours (9, 10). Indeed, many examples of biomolecular condensates, e.g. nucleolus (11) and centrosome (12), had been identified and widely known before their physical states became the subject of intense investigation (13–15).

Interestingly, proposed functions of biomolecular condensates in actual living cells seem to be correlated with their physical states (Fig. 1A), as further described in the following sections. If the condensate is dynamic with active and consistent reorganization, it tends to behave as a liquid droplet, involved in basic physiological processes. The more stable the physical state of the condensate becomes, it tends to behave more like hydrogels or aggregates. In parallel with their becoming more physically stable, we start to find more and more condensates being related to pathogenic processes, with irreversible fibrous amyloids found in various neurodegenerative diseases as typical examples. The correlation implies potential biological importance of the physical states of non-membrane-bound organelles. However, conventional techniques in cell biology are often not adequate to specifically manipulate or disturb the physical states of the condensates forming inside living cells with the level of control required. This technological challenge has hampered assessment of direct causal relationships between their physical and biological properties, a strong drive leading to recent development of novel technological paradigms (Fig. 1B and Table I).

These tools are designed to form synthetic biomolecular condensates in living cells, typically with spatial and/or temporal manoeuvrability. By synthetically harnessing certain physical states in living cells, the tools can provide significant insights into the biological roles of the physical states in defining functions of biomolecular condensates. Several tools among those

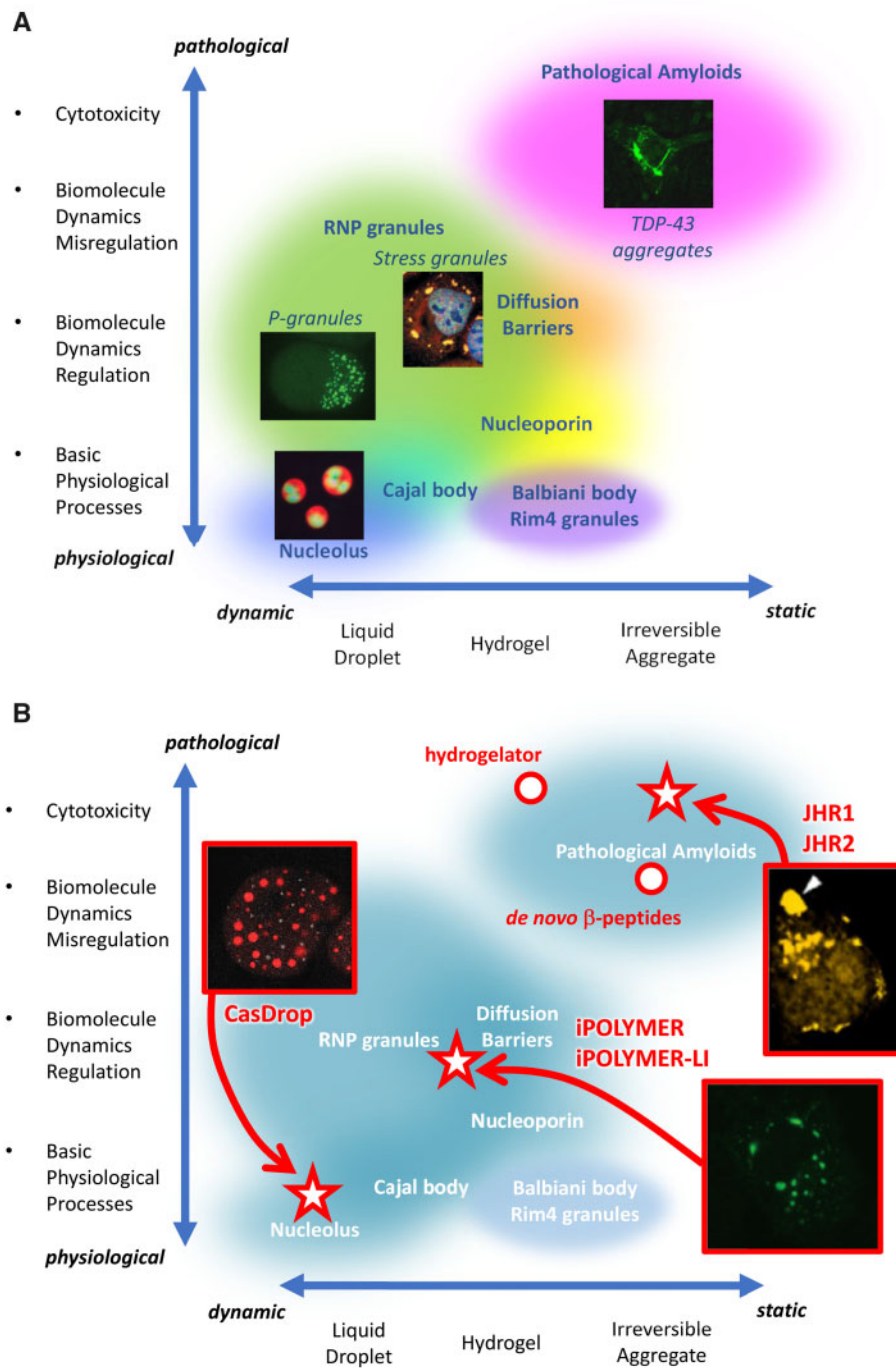


**Fig. 1 Biological roles of both endogenous and synthetic biomolecular condensates correlate with the physical states of the condensates. (A)** Proposed functions of biomolecular condensates are plotted in relation to their physical states. Balbiani body and Rim4 granules are shown together between hydrogels and irreversible aggregates due to their ‘amyloid-like’ stable natures and their basic physiological roles, although they have not been clearly attributed to any of the three physical states in the original reports (86, 87). Distinct classes of condensates are shown in distinct colours. Images of the actual condensates are shown for representative examples. Horizontal axis is the physical states that have been related to the actual biomolecular condensates, from dynamic liquid droplets to static aggregates from left to right. Vertical axis is the spectrum of biological functions ranging from basic physiological functions to pathological functions, from bottom to top. Overall distributions clearly suggest a correlation between the physical states and the functions of the novel class of intracellular structures. Images are modified from Ref. (88) (nucleolus), (89) (P-granules), (90) (stress granules), (91) (TDP-43 aggregates) with permission. **(B)** Synthetic tools that have implied a correlation between the physical states and biological functions are shown in the same scatter plot as (A). Ranges of physical state-function relations found for actual biomolecular condensates are still shown in the background for comparison. Inducible tools that can be manipulated either by chemical or light stimulus are shown as representative images taken from the original articles, while non-inducible tools are shown as red circles. Name of each tool is shown in red letters. Images are modified from Ref. (45) (CasDrop), (60) (iPOLYMER/iPOLYMER-LI), (71) (JHR1/2) with permission.

highlighted below have already succeeded in suggesting the importance of physical states in relation to relevant biological functions, as illustrated in Fig. 1B. This figure highlights the tools that have revealed the biological roles of the condensates (vertical axis) in relation to their physical states (horizontal axis), while Table I provides a more comprehensive list of the tools. Of note, the synthetic condensates produced by the tools shown in Fig. 1B appear to follow the suggested correlation between the physical states and biological functions, implying the applicability of these molecular tools for the studies of naturally occurring biomolecular condensates.

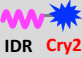


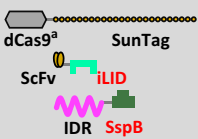
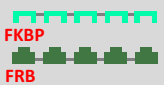






In summary, the current review offers an exhaustive list of available molecular tools for the formation of biomolecular condensates in living cells, highlighting those that are rapidly inducible, as well as studies

that characterize the physical states. Table I classifies all these tools based on three characteristics, namely, physical states, modality and design strategies illustrated in Fig. 2.

## Nature or Nurture: Physical States Commanding Functions

As mentioned above, known functions of biomolecular condensates correlate with their physical states (Fig. 1A). For example, condensates that behave like *liquid droplets* are often found in basic and house-keeping physiological contexts, e.g. processing bodies (P-bodies) (16), germ granules (17) such as P-granules found in *Caenorhabditis elegans* (18) and stress granules (19, 20) in the cytoplasm and nucleoli (21) and Cajal bodies (22) in the nucleus. These structures are

**Table I. Tools described in the current review that can form synthetic condensates in living cells**

<b>Inducible Tools</b>							
Name	Physical states	Modality	Design strategy (Class)	Schematic illustrations	Comments	Ref.	
<b>optoDroplets</b>	LD, HG, IA	Optical	I + II		<ul style="list-style-type: none"> <li>Inducibly reconstitute a wide range of physical states in a reversible manner.</li> </ul>	[40]	
<b>PixELL</b>	LD, HG	Optical	I + III		<ul style="list-style-type: none"> <li>Realize constitutive formation and inducible dissociation of the condensates.</li> <li>Spatial "memory" effect has been shown.</li> </ul>	[42]	
<b>Corelets</b>	LD, HG	Optical	I + III		<ul style="list-style-type: none"> <li>Inducible and reversible reconstitution with designed stoichiometry and improved efficiency.</li> </ul>	[43]	
<b>CasDrop</b>	LD	Optical	I + III		<ul style="list-style-type: none"> <li>Inducible reconstitution with designed stoichiometry.</li> <li>Shown to "mechanically" affect the dynamics of genetic loci to which they are targeted.</li> </ul>	[45]	
<b>iPOLYMER</b>	HG	Chemical	III		<ul style="list-style-type: none"> <li>Inducible reconstitution with designed stoichiometry.</li> <li>Shown to reconstitute stress granules <i>in situ</i>.</li> </ul>	[60]	
<b>iPOLYMER-LI</b>	HG	Optical	III		<ul style="list-style-type: none"> <li>Inducible reconstitution with designed stoichiometry in a reversible manner.</li> <li>Shown to reconstitute stress granules <i>in situ</i>.</li> </ul>	[60]	
<b>AgDD</b>	IA	Chemical	I		<ul style="list-style-type: none"> <li>Inducible formation of aggregates in living cells, as well as <i>in vivo</i> (<i>C. elegans</i>).</li> </ul>	[70]	
<b>JHR1/2</b>	IA	Optical	I		<ul style="list-style-type: none"> <li>Inducible formation of aggregates in living cells.</li> <li>Shown to be cytotoxic and to induce apoptosis.</li> </ul>	[71]	
<b>Cry2</b>	Uncharacterized	Optical	II		<ul style="list-style-type: none"> <li>Undergoes inducible oligomerization.</li> <li>Used to manipulate protein functions and/or dynamics through oligomerization of the protein fused.</li> </ul>	[41]	
<b>Cry2olig</b>	Uncharacterized	Optical	II		<ul style="list-style-type: none"> <li>Undergoes inducible oligomerization with improved efficiency.</li> <li>Used in similar ways as Cry2.</li> </ul>	[75]	
<b>Cry2clust</b>	Uncharacterized	Optical	II		<ul style="list-style-type: none"> <li>Undergoes inducible oligomerization with improved efficiency.</li> <li>Used in similar ways as Cry2.</li> </ul>	[76]	

(continued)

Table I. Continued

Non-inducible Tools						
Name	Physical States	Modality	Design Strategy (Class)	Schematic Illustrations	Comments	Ref.
PRM <sub>m</sub> + SH3 <sub>n</sub>	LD, HG	N/A	III		<ul style="list-style-type: none"> <li>Demonstrated multivalent interactions as a major mechanism of condensate formation.</li> </ul>	[39]
ArtiG	LD	N/A	III		<ul style="list-style-type: none"> <li>Used to evaluate the roles of RNA in condensate formation by RNA-binding domain fusion.</li> </ul>	[47]
Fluoppi	LD	PPI <sup>g</sup>	II + III		<ul style="list-style-type: none"> <li>Protein-protein interaction sensor utilizing condensate formation as a readout.</li> </ul>	[50]
Engineered RGG	LD	N/A	I		<ul style="list-style-type: none"> <li>Designed as a functional scaffold for protein cargo recruitment or release.</li> </ul>	[51]
Hydrogelator	HG	N/A	I		<ul style="list-style-type: none"> <li>Formation of dipeptide-based hydrogel <i>in situ</i>.</li> <li>Shown to be cytotoxic.</li> </ul>	[62]
<i>De novo</i> β-proteins	IA	N/A	II		<ul style="list-style-type: none"> <li>Structural mimicry of naturally occurring amyloids.</li> <li>Shown to mimic the cytotoxicity of amyloids.</li> </ul>	[65]
Xpa	IA (crystal)	N/A	II		<ul style="list-style-type: none"> <li>A mutant fluorescent protein that forms crystals.</li> <li>The crystals are degraded by autophagy</li> </ul>	[72]
InCell SMART-i	Uncharacterized	PPI <sup>g</sup>	III		<ul style="list-style-type: none"> <li>Protein-protein interaction sensor utilizing condensate formation as a readout.</li> </ul>	[74]

	Intrinsically Disordered Regions (IDRs)		Homodimerizing domains		Scaffold peptide with tandem binding domains
	Oligomerizing peptides (Non-IDRs)		Bait and Prey proteins		Recognizing domains
	Heterodimerizing domains		Multimerizing domains		Targeting domains

<sup>a</sup>For specific targeting of CasDrop to a certain locus, guide RNA co-expression is also required.

<sup>b</sup>Aggregate formation of AgDD is dependent on poor folding of the protein in absence of its ligand, S1. Here, we assumed therefore that the mechanism would thus be similar to that of IDRs

<sup>c</sup>IDR from an ALS-related protein, TDP-43, was conjugated to eight arginine (8R) tract via photocleavable *o*-nitrobenzyl linker.

<sup>d</sup>In living cells, tandem RGG domains formed readily visible liquid droplets, while single RGG domain did not. Taking advantage of the observation, cleavage of tandem RGGs into single RGGs by proteases was used to control the dispersal of the droplets. Protease-dependent cleavage was used also for the cargo protein release in the study.

<sup>e</sup>Precise description is C<sub>10</sub>H<sub>7</sub>CH<sub>2</sub>C(O)-phe-phe-NHCH<sub>2</sub>CH<sub>2</sub>OH, further conjugated to an esterase-cleavable butyric diacid. Hydrogel formation is dependent also on the hydrophobicity of the naphthyl group (C<sub>10</sub>H<sub>7</sub>CH<sub>2</sub>C(O)-), but we categorized the tool into Class I, due to the lack in folded peptide structure.

<sup>f</sup>The peptides were selected from a synthetic peptide library designed to share an identical pattern of alternate polar and nonpolar residues frequently found in β-strands in amyloid-forming proteins. We here categorized the tool into Class II (instead of Class I), due to the original scope of mimicking the structure of a secondary structure, β-strand.

<sup>g</sup>These tools are designed as probes to detect protein-protein interactions, rather than to synthetically form condensates. While categorized in non-inducible tools, they can readily be modified into inducible tools, e.g. using FKBP and FRB instead of bait and prey proteins, which was actually performed in both studies. Interactions between bait and prey proteins are assumed to be well characterized in terms of stoichiometry.

**Notes:** Their names, related physical states, modalities, design strategies (see main text and Fig. 2 for details), schematic illustrations of design of the peptides as well as the references describing the tool are shown. Schematic drawings include only the domains or components essential for condensate formation. For inducible tools, the components and corresponding classes of design strategy are highlighted in red. HG, hydrogel; IA, irreversible aggregate; LD, liquid droplet; N/A, not applicable; PPI, protein-protein interaction.

composed of nucleic acids and nucleic acid-binding proteins, involved in regulation of transcription or translation of the nucleic acids. The components of the droplet-like condensates undergo dynamic turnover, enabling dynamic formation, reorganization and dispersion of these structures (6–8). *Hydrogels* are another class of physical state, but with a reduced level of component turnover or dynamics compared to

liquid droplets. In their original physicochemical context, hydrogels are defined as a material with the ability to retain water when isolated from an ambient aqueous environment, and to limit molecular trafficking based on their size, besides holding certain mechanical properties (23). Examples of hydrogel-like condensates include the nuclear pore complex (24, 25), the base of primary cilia (26, 27), the assembly of myelin

membranes (28) and centrosome (12). A third class known as *insoluble aggregates* is generally long-lived and found primarily under diseased conditions, such as amyloids in neurons of neurodegenerative disease patients such as Huntington's disease, Alzheimer's disease and amyotrophic lateral sclerosis (ALS) (29). Despite the correlation between the physical states and the functions of the condensates, it is still an open question how the different physical states result in different biological outcomes.

One creative approach to addressing the question would be to synthetically fabricate intracellular structures which not only generate biomolecular condensates in living cells, but also achieve so with desired physical states without changing their molecular constituents (thus keeping the same biochemical elements). By observing the behaviour of such 'synthetic condensates', we may obtain insights into the response of cells to intracellular materials of distinct physical properties. To trace the response over time, the production of the condensates should preferably be arbitrarily manipulated through external inputs, *e.g.* chemicals or light irradiation, in an inducible manner. We categorized the 'synthetic condensates' into four physical states; liquid droplets, hydrogels, insoluble aggregates and protein clusters, the last one being a protein assembly that has not been clearly related to the other three categories.

## Molecular Tools to Harness Physical States—Modality and Design Principles

We organize the techniques based on the approach or modality used in the study (Table I), as well as on the physical states of the condensates. Studies classed as 'chemical' use small diffusible molecules to induce formation of intracellular condensates. Typical chemical tools adopt a well-established technique known as chemically induced dimerization that can induce interaction between distinct protein domains in living cells (30). 'Optical' is used to refer to tools in which condensate formation is induced by light stimulus. Optogenetic techniques are the most common examples, which utilize light-induced association between protein domains to initiate the formation. Some of these optogenetic tools have also been discussed elsewhere, focussing more on their differences in tool design strategies and on potential applications of the optogenetic tools in general (31). Tools that do not fall into either category are shown as N/A for not applicable, or with brief descriptions of the modalities adopted when needed.

It will also be useful to organize the various aggregate design strategies used in these studies (Fig. 2). Apart from practical reasons that help users adopt each tool in their research contexts, design principles of the tools should provide us with insights into the mechanisms underlying the formation of the actual biomolecular condensates encountered in living cells. Multivalent interactions between the designed molecules are the minimal requirements for the tools. Each tool described in the current review adopts

different design strategies to achieve a sufficient level of multivalency, suggesting potential diversity in the regulatory mechanisms of condensate formation. In terms of the design strategies for multivalency, all the tools listed here adopt either one of, or combinations of, three strategies, which we refer to as Classes I to III in Table I and Fig. 2. To make the tool inducible, at least one of the strategies adopted must be manipulated either by chemical or optical stimulations.

For Class I, intrinsically disordered regions (IDRs) are used to form the condensates (Fig. 2A). IDRs are defined as peptide sequences that are not likely to form a defined three-dimensional structure (32, 33). As described in many other reviews (34, 35) and in the following text, IDRs are often found in proteins forming biomolecular condensates. Also, through many *in vitro* experiments, IDRs have been demonstrated to self-assemble into macroscopic-sized condensates. It is therefore both reasonable and straightforward to adopt IDRs found in actual proteins to develop tools that form synthetic condensates in living cells. However, the physicochemical mechanisms by which IDRs form condensates are yet to be fully understood. Tools that fall into Class I can thus involve possibly unrevealed processes during the condensate formation, while the formation mechanisms are considered to resemble those of actual biomolecular condensates.

In Class II strategy, oligomerizing peptides other than IDRs are adopted (Fig. 2B). Unlike IDRs, these peptides are thought to have a certain level of defined structures, while they both share the ability to self-assemble to form macroscopic oligomers. The oligomerizing peptides are often derived from light-sensitive proteins in plants, allowing light-inducible formation of the condensates. Again, mechanisms of oligomerization are not fully understood in many cases, which should be carefully taken into account for precise interpretation of the results. One rather special case that is included in this class is a protein that tends to form a crystal, whose regular molecular order should be significantly different from those of other oligomers.

Class III strategy takes advantage of protein interactions with clearly defined stoichiometry, typically protein dimerization paradigms, to induce condensate formation (Fig. 2C). Unlike IDRs and oligomerizing peptides, dimerizing peptides cannot achieve multivalent interactions by themselves due to their well-defined one-to-one stoichiometry, demanding further measures to realize multivalency. One possible solution is to combine the strategy with the other two strategies described above. However, this solution sacrifices the significant advantage of the class over others, which is clearly defined stoichiometry of the interaction underlying the condensate formation. The other solution that can circumvent the drawback is to visibly design the valence number in the peptides. Several types of such design are adopted in the tools described below. The most straightforward is to fuse the dimerizing peptides in tandem repeats (Fig. 2C, upper panels). The number of repeats clearly defines the valency, which can be readily tuned by modifying the design. A closely related variation is to use a distinct scaffolding peptide containing tandemly repeated units, each of which

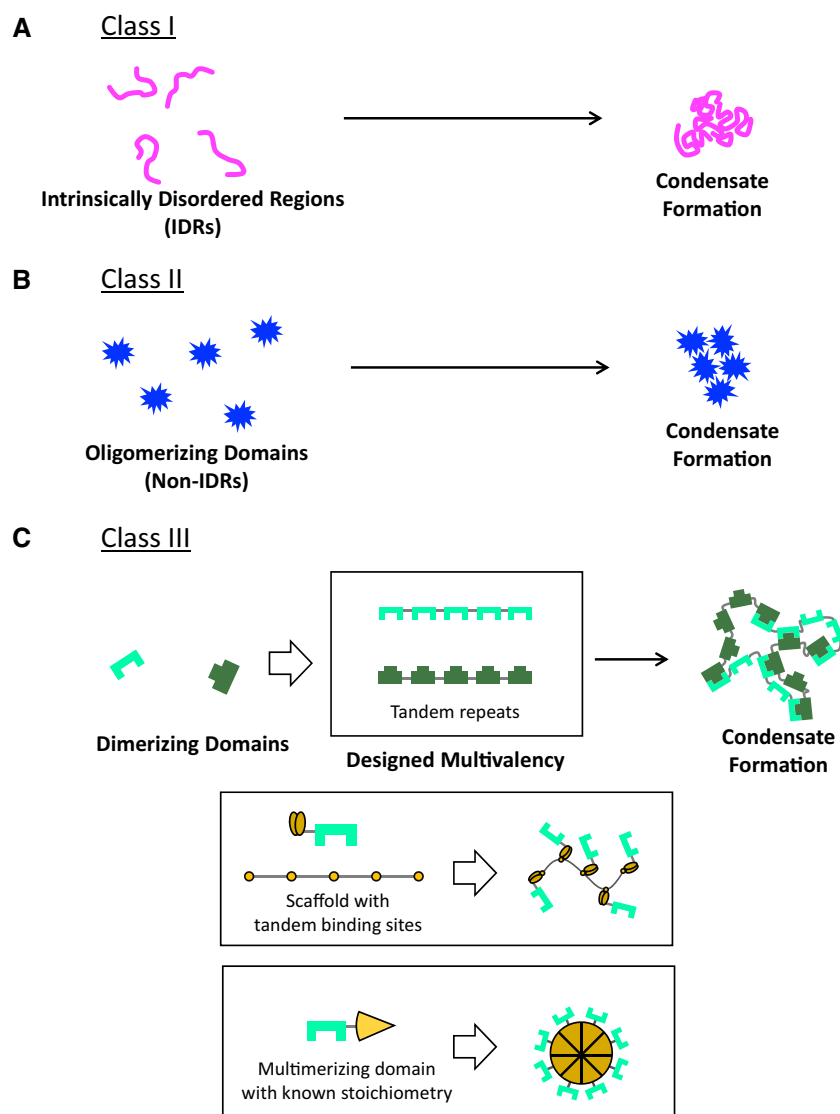


**Fig. 2 Three classes of strategies for synthetic condensate formation are shown as schematic drawings.** All the tools described in the current review adopt either one of them or multiple of them in combination to achieve multivalent interactions between the peptides. (A) Class I strategy exploits IDRs frequently found in proteins forming biomolecular condensates *in situ*. IDRs tend to form phase-separated liquid droplets or hydrogels at higher concentrations *in vivo*, suggesting the regions as a tool to synthetically form condensates in living cells. (B) Class II takes advantage of oligomerization of non-IDR proteins. These oligomerizing proteins self-assemble into condensates without clearly defined stoichiometry. Note that neither Class I nor Class II strategy involve well-defined stoichiometry. (C) In typical Class III strategy, dimerization of the peptides is used to form condensates. Due to their one-to-one binding properties, this strategy must be combined with designs that provide the tool with multivalency (designed multivalency). In the upper panel, the most straightforward design of tandem repeat dimerizing domains is depicted. A closely related design, in which independent scaffolding peptides that contain tandemly repeated binding sites for dimerizing peptides, is shown in the middle panel. In the design illustrated in the lower panel, multimerizing domains are used to form multimeric complex with the valence number determined by the stoichiometry of multimerization. Unlike the two other classes, all the designs that fall into Class III lead to rationally designed valence numbers, while performances of the additional domains or relatively large molecule sizes could possibly be disadvantageous. In Table I, this class includes a tool adopting PixD–PixE complex, which dissociates upon light irradiation.

binds to a single dimerizing peptide (Fig. 2C, middle panels). The other design involves multimerizing peptides that self-assemble with well-defined stoichiometry, which defines the valency in the design (Fig. 2C, lower panels). As a rather exceptional case, we included PixD–PixE multiprotein complex that is dissociated upon light irradiation, due to the relatively well-described stoichiometry of the complex (36, 37).

As mentioned above, the three classes of design principles are often combined to harness various physical states of the condensates described above, and in further details in the following sections. In both the text

and in Table I, the design principle(s) of each tool is shown as *e.g.* ‘Class I’, if the tool exploits only one strategy, while a description such as ‘Class I + II’ is used if it utilizes two or more strategies. In Table I, the class of design strategy that provides the tool with inducibility is highlighted in red.

## Liquid Droplets

Liquid droplets are a near-ubiquitous feature of intracellular organization. While maintaining a distinct identity in the surrounding cellular medium, liquid

droplets continue to display fluid-like properties rather than gel or aggregate features. Key features are the ability to rearrange shape, to readily fuse with other liquid droplets, rapidly exchange components with the cytoplasm and easily be deformed by flows (6). In normal cells, a number of examples of liquid droplets are known, usually involving a mixture of RNA and proteins to allow for regulation of gene expression. Examples of these ribonucleoprotein (RNP) granules include germ granules, stress granules, the nucleolus and Cajal bodies (38).

Although RNP granules are the most common examples of liquid droplet-like biomolecular condensates, one of the seminal studies in the field utilized a non-RNP granule example. Li *et al.*, in a study of the actin-associated proteins NCK and N-WASP, showed that formation of liquid droplets in cells can be explained by weak multivalent bonding between droplet components (39). They first performed *in vitro* analysis of purified repeats of the SRC homology 3 (SH3) domain of NCK and the proline-rich motif (PRM) of N-WASP, which are known to mediate association between the two proteins. A number of different combinations were tried, in the form  $\text{PRM}_m + \text{SH3}_n$ , where  $m$  and  $n$  are integers from 1 to 5 (Class III).  $\text{PRM}_5$  and  $\text{SH3}_5$  assembled into liquid droplets inside HeLa cells at concentrations of 1–10  $\mu\text{M}$ , which is within the reasonable physiological range of concentrations for native proteins. When GFP- $\text{PRM}_5$  and mCherry- $\text{SH3}_5$  were co-expressed in HeLa cells, spherical liquid droplet-like puncta formed containing both proteins; photobleaching confirmed that the droplets were highly dynamic, with turnover of the two components of under 20 s. This demonstrated the importance of multivalent tandem domain interactions in establishing liquid–liquid phase separation.

Another important mechanism of liquid droplet assembly is IDRs, which are sequences enriched in a certain subset of amino acids, typically glycine, serine, glutamine, proline, glutamic acid, lysine and arginine (7). These IDR regions are found in many proteins that form RNP liquid droplets including the ALS-associated proteins FUS, hnRNPA1 and the RNA helicase DDX4. Shin *et al.* (40) made fusions of these three IDR-containing proteins with Cry2, which oligomerizes under blue light (41). All three fusion proteins formed puncta when exposed to blue light, with the rate of puncta formation depending on both the concentration of protein and the intensity of light. The puncta exhibited properties consistent with liquid droplets, including round shape, fusion with other similar puncta and rapid fluorescence recovery after photobleaching (FRAP). They termed this system ‘optoDroplets’ (Class I + II). The authors thus demonstrated the importance of clustering of IDR motifs in establishing liquid droplets in living cells.

Relatively simple and straightforward design of optoDroplets have allowed the same group of authors to develop several recent variations with different features. Dine *et al.* (42) developed an ‘inverse’ tool, PixELL (Class I + III), that can inducibly disassemble the droplet-like condensates. The authors used two proteins, PixD and PixE, that in the dark associate

into large multi-subunit complexes, which dissociate into PixD dimers and PixE monomers upon light stimulus (36, 37). In the report, the two tools, optoDroplet and PixELL, suggested that synthetically formed liquid droplets can retain a spatial ‘memory’ of previous droplet formation. Bracha *et al.* (43) have recently reported a further advance in controlling liquid–liquid phase behaviour in living cells. Their optogenetic system, ‘Corelets’ (Class I + III), is based on a self-assembling core of 24 ferritin heavy chain subunits fused to iLID to create a spherical particle of 12-nm diameter. Blue light is then used to induce SspB-fused IDR proteins to assemble at the Corelet particle and create a liquid droplet, taking advantage of the light-induced binding between the two peptides, iLID and SspB (44). While the overall cellular concentration of IDR proteins is low, thus preventing their spontaneous global self-assembly, the presence of a freely diffusible nucleation core allows the local concentration of IDR to cross the threshold for self-assembly and create a liquid droplet. The authors suggest that a similar mechanism may be important for phase transitions involving nucleic acids, such as chromatin compaction and transcriptional control, as nucleic acids often show low diffusion rates and could act as a scaffold for multiple IDR proteins simultaneously. Another variation, ‘CasDrop’ (Class I + III), was developed by adopting dCas9 to target the liquid droplet-like condensates to a certain target gene locus (45). The condensate formation was induced by light-inducible iLID-SspB dimerization as well, while multiple iLIDs, which were associated with dCas9 by single-chain variable fragment antibody (ScFv)-based tagging system named SunTag (46), play the role of the assembling core. Through several experiments, the authors revealed that the liquid droplet-like condensates can ‘both sense and restructure their local genomic environment’. The system thus implied that the liquid droplet-like nature of intracellular biomolecular condensates, *e.g.* nucleolus, is actually essential in the regulation of the genome.

In a recently shared preprint, Garcia-Jove Navarro *et al.* (47) developed a versatile scaffold, ArtiGranule or ArtiG (Class III), that behaves as liquid droplets. The design involves homodimerization of mutant FKBP protein, F36M-FKBP (48), and human ferritin that forms a 24-mer, without any IDRs. The authors further fused an RNA-binding domain, Pumilio homology domain, with the tool to recruit RNA to the condensate, suggesting the active roles of RNA in droplet-like condensate formation. RNA had already been demonstrated to form hydrogels *in vitro* without any involvement of proteins (49), which suggests potentially important roles of the molecular species in biomolecular condensate formation. Synthetic liquid-like condensate can thus be used to examine the mechanism of biomolecular condensate formation *in situ*.

Studies on liquid droplet-like condensates are not necessarily limited to basic biological interest in the behaviour of physiological condensates. A recent study by Watanabe *et al.* exploits liquid–liquid phase separation as a tool to determine protein–protein interactions (PPIs) in cells (50). When the oligomeric

fluorescent protein Azami-Green and the p62 PB1 domain were fused to proteins of interest and co-expressed in cells, liquid droplet-like puncta were observed if the two proteins showed interaction with each other. This technique was thus termed Fluoppi (fluorescent protein–protein–interaction–visualization) (Class II + III). The puncta were further confirmed to display liquid droplet behaviour such as fusing with each other in living cells. Fluoppi succeeded in monitoring rapid and reversible PPIs in living cells. The authors also demonstrated Fluoppi in high content drug screening to analyse drug-induced PPI blockage. Then, Azami-Green was replaced with a novel photoconvertible protein, Momiji, to develop photoconvertible Fluoppi, or pcFluoppi. It could then be used to study the kinetics of PPIs, due to its optical highlighting feature. Fluoppi thus stands as a useful tool for probing PPIs that relies on liquid drop formation in cells.

A recent study by Schuster *et al.* (51) utilized an artificial liquid droplet based on engineered LAF-1 RGG domains (52) to recruit or release protein cargos (Class I). The recruitment of cargos was realized by dimerization of a synthetic coiled-coil pair SYNZIP (53), while their release was controlled via protease-dependent enzymatic cleavage of tandem RGG domain-containing peptides. The result implied the promise of synthetic condensates as a scaffold to nucleate arbitrary biochemical reactions in biotechnological applications.

## Hydrogels

A hydrogel is a hydrophilic polymer network that contains a high degree of water and considerable mechanical elasticity (23). Hydrogels are distinct from liquid droplets in demonstrating much less exchange of their components with the environment and little internal motion of constituent molecules. While hydrogels appear to be less ubiquitous in nature than liquid droplets, examples are known in established intracellular structures including the nuclear pore complex and the centrosome, as well as in structures whose molecular identities are yet to be revealed, such as myelin sheath assembly and the diffusion barriers at the base of primary cilia. These structures are typically modulating the dynamics of diverse biomolecules, maintaining their physiological intracellular localizations. Physical properties of the hydrogels, *e.g.* effective pore size, turnover dynamics and viscoelasticity, are thus considered to be essential for their functions through physical interactions with the target biomolecules. Despite the difficulties in demonstrating physical states in living cells, phenylalanine-glycine (FG) repeats in nucleoporins are one of the best-studied among these examples. In a series of elegant studies, purified FG-repeat peptides formed well-defined macroscopic hydrogels *in vitro*, successfully reproducing the selective permeability of nuclear pores (24, 25, 54, 55).

Hydrogels have also been related to condensates whose physical states are primarily categorized as liquid droplets or as irreversible aggregates. Two key papers in this context were published from the same

group in 2012, reporting intrinsically disordered domains found in diverse RNA-binding proteins formed hydrogels *in vitro* (56, 57). Among the RNA-binding proteins, TIA-1 is an established component of a class of RNP granule, stress granules, while FUS and TDP-43 are known to be involved in neurodegeneration, forming irreversible aggregates in diseased cells. Both liquid droplet-like RNP granules and neurotoxic irreversible aggregates are thus associated with hydrogels, suggesting the physical state as a hub connecting the two other states, liquid droplets and aggregates. Two recent studies further pursued the perspective by taking into account FUS gene mutations found in neurodegenerative disease patients; Patel *et al.* (58) first found that ALS-related protein, FUS, forms liquid droplet-like condensates in living cells upon various stresses. They further established an *in vitro* experiment, in which purified FUS protein forms dynamic liquid droplets. When highly concentrated, FUS protein also formed hydrogel *in vitro*. The authors then tested mutants of FUS, G156E and R244C, which had been reported in ALS patients, in the liquid droplet setup. The authors compared the mutants with wild-type FUS and found that these mutations accelerate the ‘aging’ of droplets into fibrillar aggregates over time. In another study, Murakami *et al.* (59) also analysed wild-type as well as ALS-associated mutants of FUS, both in living cells and *in vitro*. They also found that the mutations reduced the reversibility of liquid droplets formed by the proteins. Based on viscosity measurement and electron microscopy, the authors concluded that the reduced reversibility states were hydrogels. They further revealed that the irreversible hydrogels result in decreased protein synthesis in neurons. The authors suggest that the mutant forms of FUS may have impaired ability to release their RNP cargoes, due to the irreversible hydrogels they form, thus providing a potential mechanism for how mutations causing hydrogel formation in neuronal cells could lead to the neuronal damage observed in ALS patients.

These previous studies suggest the importance of hydrogels in biologically and clinically relevant situations, in close relation to other physical states associated with biomolecular condensates, *i.e.* liquid droplets and irreversible aggregates. On the other hand, these results highlighted the challenge in identifying a certain condensate as a well-defined hydrogel in living cells. Most studies relied only upon *in vitro* reconstitution experiments to identify the condensates as hydrogels, and conclusions from distinct groups may vary according to the details of the experiments. Preferably, therefore, a tool that reconstitutes a hydrogel in living cells should provide evidence for the identity of the condensate as a hydrogel both *in vitro* and in living cells.

Nakamura *et al.* (60) recently published a study, in which they managed to meet the demand to a certain extent. The authors succeeded in inducing the formation of hydrogels in living cells using both a chemically induced dimerization system and an optogenetic system. Fusion proteins of fluorescent protein linked to between 1 and 5 repeats of either FKBP or FRB



were co-transfected into cells, and the chemical dimerizer rapamycin was added. Formation of the hydrogel was shown to be valence-dependent, with a larger fraction of cells containing puncta for higher valence numbers. Unlike liquid droplets, these puncta were irregular in shape with little morphological reorganization, and showing very little recovery of fluorescence after photobleaching. The puncta *in situ* also showed a 'sieve-like' feature characteristic of hydrogels in allowing through molecules and small particles but not larger particles such as trans-Golgi vesicles. These behaviours resembled the well-defined hydrogels formed by the purified polypeptides *in vitro*, suggesting the identity of the puncta observed *in situ* as hydrogels. The authors termed this system iPOLYMER (Class III). The significance of the technique lies in its design of well-defined and tuneable valencies of the polypeptide chains. Indeed, iPOLYMER with distinct valence numbers of both polypeptides demonstrated the essential effects of valencies in *in situ* hydrogel formation. A reversible optogenetic system, called iPOLYMER-LI (for 'light inducible'), was also constructed by using iLID and its binding partner SspB in place of FKBP and FRB (Class III). When the iPOLYMER or iPOLYMER-LI gel was functionalized by fusing the RNA recognition motif of RNA granule protein to the polypeptide chains, the hydrogel acted as an artificial RNA granule, and known stress granule proteins were found to associate to the iPOLYMER gels in living cells. This ability to reconstitute a non-membrane-bound organelle in living cells may be of great interest in further studies.

Shin *et al.*, in their previously referenced study, also were able to make hydrogels in living cells under certain circumstances (40). By varying the intensity of light to optoFUS cells, they were able to shift the location of the molecule on the saturation chart. At low light intensities, liquid droplet-like aggregates were formed; however, at the highest light intensities which pushed the molecules into 'deep supersaturation', more gel-like aggregates were formed. These gel-like aggregates showed more irregular shapes, poor recovery after photobleaching and fewer cycles of light/dark assembly/disassembly before the formation of small insoluble patches that can no longer dissociate. In the study, identity of the aggregate as a hydrogel is thus primarily supported by morphology and dynamics of protein turnover, which may technically fall short as a stringent definition of a hydrogel. However, judging from a wide variety of evidence that relates IDRs to hydrogels, these results successfully serve to illustrate the close connection between liquid droplet formation and hydrogel formation in living cells; the same molecules may participate in either type of structure, depending on local conditions within the cell. The concept had been implied in previous studies (58, 59, 61), but was clearly demonstrated in living cells for the first time in the study.

One further report of hydrogel formation in living cells bears mention, due to its clear reference to the biological effects of the synthetic condensate. Yang *et al.* (62) designed an artificial substrate consisting of a hydrophobic naphthyl group to enhance self-assembly

in aqueous environments, a dipeptide segment (phe-phe) as acceptor and donor of hydrogen bonds and an esterase-cleavable butyric diacid. When added to culture medium with HeLa cells, the substrate is taken up by the cells, at which point an intracellular esterase cleaves the butyric diacid, releasing the active hydrogelator (Class I). The hydrogelator molecule then self-assembles into nanofibers, which form a hydrogel-like structure and, over a period of hours to days, leads to cell death. While this does constitute production of an artificial nanostructure inside a living cell, the relevance to physiological hydrogel formation is unclear at this moment.

## Insoluble Aggregates

Insoluble protein aggregates, *e.g.* aggregates of misfolded proteins, are swiftly targeted for degradation in healthy cells (63). In contrast, longer-lived protein aggregates are found in several disease conditions including neurodegenerative diseases, thus of considerable interest. The aggregates typically exhibit highly ordered fibrillar states, with component  $\beta$ -strands oriented perpendicularly to the fibril axis, often referred to as amyloid or prion-like in the context (64). These insoluble aggregates are one of the clearest symptoms of the diseases, naturally drawing attention in many previous studies (27). Despite intense investigations, the mechanisms by which these aggregates exert their toxic effects to the cell are yet to be fully elucidated.

This situation is, at least in part, due to the methodology adopted in previous reports. Many conventional studies tried to address the possible toxicity of intracellular protein aggregates simply by overexpressing proteins that form aggregates in diseased cells. However, different pathophysiological proteins often have different characters, such as intracellular distributions, and different biological functions besides forming aggregates, making the results rather difficult to interpret.

An ideal solution to understand the mechanism of toxicity would be to develop *de novo* synthetic peptides that form aggregates in living cells, based on the common features of various pathological proteins. Indeed, as early as 1999, West *et al.* published a paper on such a trial (65); the authors constructed a combinatorial library of *de novo* peptides of multimeric  $\beta$ -strands, trying to mimic the periodicity of polar and nonpolar residues in the sequence, which is common among the proteins destined to assemble into aggregates. Eight proteins arbitrarily chosen from the library were expressed in *Escherichia coli* and purified, then subject to *in vitro* evaluation to test self-assembly. As a result, all eight peptides were shown to form oligomers with  $\beta$ -sheet secondary structure in a reversible manner (Class II). Furthermore, these synthetic amyloids were readily stained by Congo red, a chemical dye commonly used for diagnostics to detect the presence of amyloids. These results demonstrate the promise of these rationally designed *de novo* synthetic peptides.

Two recent key studies adopted above-mentioned synthetic peptides as model aggregate-forming

proteins, revealing distinct mechanisms for the toxicity of protein aggregates. Olzscha *et al.* (66) confirmed that overexpression of the  $\beta$ -strand peptides in mammalian cells caused cytotoxicity over several days. The authors then performed quantitative proteomic analysis of the  $\beta$  protein interactome using SILAC and LC-MS/MS. The interactors identified shared distinct physicochemical properties, including the large size and enriched unstructured or disordered regions. They often occupied essential hub positions in protein interaction networks, with key roles in various essential events such as chromatin organization, transcription/translation, cell architecture maintenance and protein quality control. The authors further performed pulse-SILAC experiments and concluded that the interactor proteins can be classified into two overlapping subsets: One group is enriched in IDRs, and prone to aggregate by its nature. The other group consists of relatively large sized proteins which require longer times for synthesis and folding, during which they tend to be sequestered by the synthetic aggregates. This report thus proposed that the amyloidogenic protein aggregation targets a 'metastable subproteome', thereby causing toxicity via a wide variety of essential cellular processes.

The other study adopting the *de novo* synthetic  $\beta$ -proteins focussed on a specific mechanism of the toxicity, which is nucleocytoplasmic transport. Deficient nucleocytoplasmic transport had previously been reported in cells with the hexanucleotide repeat expansion in the C9orf72 gene, which is the most common cause of ALS (67, 68). Woerner *et al.* (69) successfully confirmed the involvement of insoluble protein aggregates in the deficiency, using *de novo*  $\beta$ -protein aggregate, as well as two peptides derived from pathological proteins, TDP-43 and huntingtin, as a model. The use of synthetic peptides allowed the authors to propose the universality or sequence-independency of the results in a convincing manner. Furthermore, the authors discovered that the effects of protein aggregates on nucleocytoplasmic transport were dependent on the location of the aggregates; when they are formed in the nucleus, there was little effect on transport, while cytosolic aggregates significantly attenuated the nucleocytoplasmic transport. The authors took advantage of the synthetic aggregate-forming peptides by simple and straightforward engineering, revealing a basic understanding of the toxicity. Interestingly, actual pathological insoluble protein aggregates can be found in the nucleus, as well as in the cytosol, posing the roles of nuclear aggregates as an intriguing open question.

*De novo*  $\beta$ -proteins have thus been successful in elucidating the mechanisms through which intracellular insoluble protein aggregates exert their toxicity. However, relatively poor temporal resolution of the technique limits its application in elucidating temporal evolution or maturation of the aggregates. Indeed, in multiple previous reports described above (58, 59), it is suggested that toxic insoluble protein aggregates are initially formed as liquid droplet or hydrogel, followed by gradual conversion into toxic aggregates or a 'maturation' process. Understanding of the maturation

process, also referred to as aberrant phase separation, over time would thus be fundamental in the context. For the purpose, aggregate-forming peptides with higher temporal resolution, or rapidly inducible aggregate-formation techniques, would be suitable.

Miyazaki *et al.* (70) report a method, termed AgDD (Class I), to rapidly induce protein aggregates inside living cells. AgDD is based on a previously published destabilization domain derived from FKBP12 protein. In the absence of its ligand S1, AgDD rapidly unfolds, leading to destabilization of associated protein domains which can then form aggregates. AgDD-expressing HEK293T cells were grown in media containing the S1 ligand; cells were then shifted to S1-free media for 150 min, leading to aggregation of the AgDD into small puncta which aggregate over time. Formation of these puncta is reversible by adding S1 back into the media. AgDD aggregates were shown to behave like known filamentous aggregated proteins such as the  $\Delta$ F508 mutant of cystic fibrosis transmembrane conductance regulator. One important achievement of the study is successfully inducing generation of the aggregates *in vivo*, as demonstrated by the experiment using *C. elegans* intestine. This inducible and reversible method for creating protein aggregation may thus be of use in studying clinically relevant protein aggregates.

He *et al.* (71) developed an inducible system in which they engineered a domain from pathological protein TDP-43 to obtain a photocontrollable probe, JHR1 and JHR2, which differ in molecular tags for detection (Class I). Their study is in the line of previous research aiming at inducible aggregate- or amyloid-forming peptides out of the actual peptides found in relevant diseases. The novelty of the paper is that they developed a technique which can rapidly induce the amyloid formation both *in vitro* and *in situ*, unlike previous reports focussed on characterization of amyloid formation process *in vitro*. For the purpose, the authors used two components, eight-arginine tract (8R) and *o*-nitrobenzyl photocleavable linker. The 8R tract performs two key functions in their design: it provides the probe with cell-penetrating ability, and also with condensed positive charges that prevent self-aggregation of TDP-43-derived peptide. The probe, which is Alexa dye-labelled TDP-43 C-terminal amyloidogenic sequence and the 8R tract conjugated by an *o*-nitrobenzyl linker, does not form aggregates in solution due to the 8R tract. When the probe is administrated extracellularly, the 8R tract allows the probe to penetrate into the cytosol. Upon UV irradiation, *o*-nitrobenzyl linker is rapidly cleaved, allowing TDP-43 peptide to self-assemble into amyloids *in situ*. The authors confirmed that the probe induced amyloid formation both *in vitro* and in living cells. They further confirmed the toxicity of the amyloid produced by the probe in primary neurons. Of note, TDP-43 pathological aggregates from diseased brains are reported to function as seeds to induce further TDP-43 aggregation in other cells. This prion-like behaviour is also maintained in the inducible probe, as is confirmed in the publication.

Toxic protein aggregates or amyloids often share a certain level of structural order, as described earlier. The extent to which the aggregate is structurally ordered may thus be an essential aspect of the toxicity caused by protein aggregates. One extreme example of the structural order synthetically realized in a living cell can be found in Tsutsui *et al.* (72). The authors made variants of a photoconvertible fluorescent protein, KikGR (73), to obtain a variety, Xpa, which formed crystals when expressed in mammalian cells (Class II); these crystals were on the scale of several microns, and were sufficient to allow X-ray crystallographic determination of the protein structure to a resolution of 2.9 angstroms. These crystals were targeted to lysosomes for degradation, recognized as a lysosomal target. As protein crystal formation is observed in natural processes such as protein storage in plant seeds, this finding may be of use in studying such processes.

## Protein Clustering

Apart from the context of phase behaviour-related biomolecular condensates, it has been generally accepted that protein clustering is widespread in cells and is crucial in modulating various signal transduction pathways. By locally concentrating specific proteins, clustering allows highly spatially and temporally localized activity within the cell. Several studies have attempted to reproduce protein clustering in living cells and to use experimentally induced clustering as a tool to study PPIs. The precise physical nature of the clusters (*i.e.* liquid droplet, hydrogel or insoluble aggregate) was not of the authors' interest in the original context, and often was not pursued. We therefore classify the protein clusters formed by the techniques below as 'uncharacterized' in Table I. However, significance of the studies in the context of biomolecular condensates should never be underestimated; the techniques described so far are often developed based on protein clustering techniques shown below. The tools described below thus paved the way to synthetic biological approaches to biomolecular condensates. Also, the mechanisms by which the tools work are thus fundamental in interpreting the results obtained.

Early work in this line was published in 2011 by Lee *et al.* (74). Their system, InCell SMART-i, is based on fluorescently labelled self-assembling ferritin nanoparticles which are fused to 'bait' and 'prey' proteins (Class III). If the bait and prey proteins interact with each other, the nanoparticles assemble into roughly circular clusters with areas of over  $0.2 \mu\text{m}^2$ . This was verified with FKBP and FRB as bait and prey, with rapamycin addition necessary to see interaction between the two molecules. The InCell SMART-i technique was also verified for the NF- $\kappa$ B pathway in cells. The technique is suggested to be broadly applicable in detecting PPIs inside living cells. The claim was further confirmed by the successful development of another PPI sensor described earlier, Fluoppi, that exploits a similar design principle, but with clearer reference to the liquid droplet-like behaviour of the condensates (50).

Several groups have reported success in inducing protein clustering via optogenetics. Bugaj *et al.* (41) took advantage of the inherent clustering ability of Cry2 upon stimulation with blue light (488-nm wavelength), even without its usual dimerization partner CIB1 (Class II). They were able to induce small clusters of proteins both in the cytoplasm and at the cell membrane in a reversible fashion. This Cry2-based clustering was then used in HEK293T cells to relieve  $\beta$ -catenin inhibition (by clustering the negative regulatory domain LRP6c) and to induce actin cytoskeletal reorganization (by clustering RhoA at the cell membrane and vesicles). Taslimi *et al.* (75) reported a mutant form of Cry2 that they termed Cry2olig (Class II). Cry2olig showed greatly enhanced self-oligomerization upon blue light stimulation compared to native Cry2 protein. Cry2olig was then used to cross-link clathrin light chain, thus disrupting clathrin-dependent endocytosis. Actin assembly was also perturbed using Cry2olig fused to the SH3 domain of the actin nucleating protein Nck. This resulted in actin assembly and, with prolonged (over 1 h) exposure to blue light, cell shape changes due to loss of focal adhesion-actin connections. In the same report, the authors also utilized Cry2olig as the basis for two techniques, LINC and LINC-FRAP, which can evaluate PPIs in living cells. A further refinement of the Cry2 optogenetic system, termed Cry2clust (Class II), was reported by Park *et al.* (76). Cry2clust was shown to exhibit faster assembly and disassembly kinetics than other Cry2 clustering tools, and to produce larger average cluster sizes in both nucleus and cytoplasm.

Cry2 clustering tools are adopted as building blocks of several inducible systems described in previous sections. Understanding the mechanism of Cry2 or improved versions of Cry2 clustering can thus be essential in interpreting the results in those studies. One such example can be seen in the optoDroplets study described above (40); the use of Cry2olig instead of Cry2 lead to slower molecular turnover demonstrated by FRAP measurement. The authors interpreted the slower FRAP kinetics as demonstrating a more 'gel-like' property. However, it would be worth pointing out that the FRAP kinetics of the clustered or oligomerized Cry2olig on its own, without any IDR, is already similarly slow in their data. The interpretation of the role of IDRs in the context should thus be carefully examined, taking the nature of the clustering tools adopted in the study into account.

## Discussions and Prospects

The molecular tools described above are now readily applicable to many biological experiments to garner insights into the organization and function of intracellular biomolecular condensates that had been out of reach by conventional methodology alone. For example, minimal requirements for the molecular identity of each biomolecular condensate could be elucidated by synthetic reconstitution of the condensate, combining the synthetic tools and molecules of interest to be assembled. This idea has already been

partially pursued in two studies described above (47, 60), with distinct RNA-binding domains fused to the tools, ArtiG and iPOLYMER/iPOLYMER-LI, respectively. Another interesting research suggests a spatial ‘memory’ of droplet formation (42). Although the mechanism is yet to be demonstrated, the simple memory effects based on protein phase separation may underlie certain biological phenomena that are not well understood so far.

Beyond the roles of the physical status of the condensates, these tools may be of use in tackling many open questions in the field. One intriguing question is the maturation process of insoluble aggregates. As suggested in several studies (58, 59), insoluble aggregates seem to undergo a maturation process through which they become irreversible and gain toxicity. However, it is still unclear what exactly happens during the maturation process, both physicochemically and biologically, especially in actual living cells. A series of studies described in the current review successfully suggested the continuum of three physical states in living cells (40, 43), but the mechanisms underlying the maturation or aging in the states are yet to be elucidated. Manipulation of the process at a precisely intended timing should reveal the temporal evolution of the aggregates. Another open question is the crosstalk between distinct biomolecular condensates. Previous studies reported a functional crosstalk between distinct biomolecular condensates in different biological contexts including mRNA processing (77), epigenetic inheritance (78) and neurodegenerative diseases (79–82). The tools to manipulate the formation of biomolecular condensates may reveal the rules underlying the ‘sociology of biomolecular condensates’.

Despite the promise listed above, there is still plenty of room for improvement of these tools. First, their performance is not always robust enough, especially when combined with bulk or comprehensive analyses including biochemistry and omics approaches. The use of these tools is thus often limited to single-cell studies, in combination with microscopy analyses. Also, unbiased benchmarking test for the tools has yet to be established as well as technically challenging. New users thus have to go through considerable trials and errors to find the best tool for their purposes. Second, except for several remarkable examples, these tools have not been demonstrated in realistic biological environments, or in model animals. Capability to actuate these tools ‘*in vivo*’ would become significant, especially in the context of neurodegenerative diseases where output phenotypes associate with ensembles of neurons and other types of cells such as glia and muscles. Third, in terms of the molecular constituents, most of the current tools concern actuation of proteins, rather than equally important counterparts, namely RNAs (47, 49, 83–85), necessitating future development of tools for RNA assembly.

It is worth mentioning that clearly defined thresholds in terms of dynamic behaviours between hydrogels and liquid droplets, or hydrogels and insoluble aggregates, are currently missing. As a consequence hydrogel-like biomolecular condensates are often referred to condensates with ‘intermediate’ properties

between liquid droplets and insoluble aggregates. For biologists, these properties include molecular turnover and reorganization of the overall morphology, while materials scientists preferentially consider mechanical properties. The ambiguity may seem trivial, but could hamper growth of this inherently interdisciplinary research subject. It is thus imperative to have a consensus on their terminology with clear definition.

Studies on the unique, membrane-less intracellular organization such as biomolecular condensates have just been launched. Another development we urgently need includes an inducible method for disassembly or alteration of physical states of ‘native’ condensates, again, in a living cell setting. Toward this end, multidisciplinary collaborations among biologists, physicists, materials scientists and others continue to be vital.

## Acknowledgements

We would like to apologize to the researchers whose work could not be cited or referenced due to the limited space of the current review. We thank Geraldine Seydoux for helpful discussions, critical reading of the manuscript and writing suggestions.

## Funding

This work was supported by the US National Institutes of Health grant (GM123130) and Mirowski Discovery Award Fund to TI.

## References

- Banani, S.F., Lee, H.O., Hyman, A.A., and Rosen, M.K. (2017) Biomolecular condensates: organizers of cellular biochemistry. *Nat. Rev. Mol. Cell Biol.* **18**, 285–298
- Hnisz, D., Shrinivas, K., Young, R.A., Chakraborty, A.K., and Sharp, P.A. (2017) A phase separation model for transcriptional control. *Cell* **169**, 13–23
- Sabari, B.R., Dall’Agnese, A., Boija, A., Klein, I.A., Coffey, E.L., Shrinivas, K., Abraham, B.J., Hannett, N.M., Zamudio, A.V., Manteiga, J.C., Li, C.H., Guo, Y.E., Day, D.S., Schuijers, J., Vasile, E., Malik, S., Hnisz, D., Lee, T.I., Cisse, I.I., Roeder, R.G., Sharp, P.A., Chakraborty, A.K., and Young, R.A. (2018) Coactivator condensation at super-enhancers links phase separation and gene control. *Science* **361**, eaar3958
- Riback, J.A., Katanski, C.D., Kear-Scott, J.L., Pilipenko, E.V., Rojek, A.E., Sosnick, T.R., and Drummond, D.A. (2017) Stress-triggered phase separation is an adaptive, evolutionarily tuned response. *Cell* **168**, 1028–1040.e19
- Aguzzi, A. and Altmeyer, M. (2016) Phase separation: linking cellular compartmentalization to disease. *Trends Cell Biol.* **26**, 547–558
- Hyman, A.A., Weber, C.A., and Jülicher, F. (2014) Liquid–liquid phase separation in biology. *Annu. Rev. Cell Dev. Biol.* **30**, 39–58
- Shin, Y. and Brangwynne, C.P. (2017) Liquid phase condensation in cell physiology and disease. *Science* **357**, eaaf4382
- Boeynaems, S., Alberti, S., Fawzi, N.L., Mittag, T., Polymenidou, M., Rousseau, F., Schymkowitz, J., Shorter, J., Wolozin, B., Van Den Bosch, L., Tompa, P., and Fuxreiter, M. (2018) Protein phase separation: a new phase in cell biology. *Trends Cell Biol.* **28**, 420–435

9. Walter, H. and Brooks, D.E. (1995) Phase separation in cytoplasm, due to macromolecular crowding, is the basis for microcompartmentation. *FEBS Lett.* **361**, 135–139
10. Toretzky, J.A. and Wright, P.E. (2014) Assemblages: functional units formed by cellular phase separation. *J. Cell Biol.* **206**, 579–588
11. Brangwynne, C.P., Mitchison, T.J., and Hyman, A.A. (2011) Active liquid-like behavior of nucleoli determines their size and shape in *Xenopus laevis* oocytes. *Proc. Natl. Acad. Sci. USA* **108**, 4334–4339
12. Woodruff, J.B., Ferreira Gomes, B., Widlund, P.O., Mahamid, J., Honigsmann, A., and Hyman, A.A. (2017) The centrosome is a selective condensate that nucleates microtubules by concentrating tubulin. *Cell* **169**, 1066–1077.e10
13. Pederson, T. (2011) The nucleolus. *Cold Spring Harb. Perspect. Biol.* **3**, a000638
14. Scheer, U. (2014) Historical roots of centrosome research: discovery of Boveri's microscope slides in Würzburg. *Philos. Trans. R. Soc. Lond. B* **369**, 20130469
15. McIntosh, J.R. and Hays, T. (2016) A brief history of research on mitotic mechanisms. *Biology* **5**, 55
16. Luo, Y., Na, Z. and Slavoff, S.A. (2018) P-Bodies: composition, properties, and functions. *Biochemistry* **57**, 2424–2431
17. Sengupta, M.S. and Boag, P.R. (2012) Germ granules and the control of mRNA translation. *IUBMB Life* **64**, 586–594
18. Seydoux, G. (2018) The P granules of *C. elegans*: a genetic model for the study of RNA-protein condensates. *J. Mol. Biol.* **430**, 4702–4710
19. Kedersha, N., Ivanov, P., and Anderson, P. (2013) Stress granules and cell signaling: more than just a passing phase? *Trends Biochem. Sci.* **38**, 494–506
20. Protter, D.S.W. and Parker, R. (2016) Principles and properties of stress granules. *Trends Cell Biol.* **26**, 668–679
21. Nemeth, A. and Grummt, I. (2018) Dynamic regulation of nucleolar architecture. *Curr. Opin. Cell Biol.* **52**, 105–111
22. Machyna, M., Heyn, P., and Neugebauer, K.M. (2013) Cajal bodies: where form meets function. *Wiley Interdiscip. Rev. RNA* **4**, 17–34
23. Hoffman, A.S. (2002) Hydrogels for biomedical applications. *Adv. Drug Deliv. Rev.* **54**, 3–12
24. Frey, S., Richter, R.P., and Görlich, D. (2006) FG-rich repeats of nuclear pore proteins form a three-dimensional meshwork with hydrogel-like properties. *Science* **314**, 815–817
25. Frey, S. and Görlich, D. (2007) A saturated FG-repeat hydrogel can reproduce the permeability properties of nuclear pore complexes. *Cell* **130**, 512–523
26. Breslow, D.K., Koslover, E.F., Seydel, F., Spakowitz, A.J., and Nachury, M.V. (2013) An in vitro assay for entry into cilia reveals unique properties of the soluble diffusion barrier. *J. Cell Biol.* **203**, 129–147
27. Lin, Y.-C., Niewiadomski, P., Lin, B., Nakamura, H., Phua, S.C., Jiao, J., Levchenko, A., Inoue, T., Rohatgi, R., and Inoue, T. (2013) Chemically inducible diffusion trap at cilia reveals molecular sieve-like barrier. *Nat. Chem. Biol.* **9**, 437–443
28. Aggarwal, S., Snaidero, N., Pähler, G., Frey, S., Sánchez, P., Zweckstetter, M., Janshoff, A., Schneider, A., Weil, M.-T., Schaap, I.A.T., Görlich, D., and Simons, M. (2013) Myelin membrane assembly is driven by a phase transition of myelin basic proteins into a cohesive protein meshwork. *PLoS Biol.* **11**, e1001577
29. Ross, C.A. and Poirier, M.A. (2004) Protein aggregation and neurodegenerative disease. *Nat. Med.* **10** Suppl., S10–S17
30. DeRose, R., Miyamoto, T., and Inoue, T. (2013) Manipulating signaling at will: chemically-inducible dimerization (CID) techniques resolve problems in cell biology. *Pflugers Arch.* **465**, 409–417
31. Dine, E. and Toettcher, J.E. (2018) Optogenetic reconstitution for determining the form and function of membraneless organelles. *Biochemistry* **57**, 2432–2436
32. Uversky, V.N. and Dunker, A.K. (2010) Understanding protein non-folding. *Biochim. Biophys. Acta* **1804**, 1231–1264
33. van der Lee, R., Buljan, M., Lang, B., Weatheritt, R.J., Daughdrill, G.W., Dunker, A.K., Fuxreiter, M., Gough, J., Gsponer, J., Jones, D.T., Kim, P.M., Kriwacki, R.W., Oldfield, C.J., Pappu, R.V., Tompa, P., Uversky, V.N., Wright, P.E., and Babu, M.M. (2014) Classification of intrinsically disordered regions and proteins. *Chem. Rev.* **114**, 6589–6631
34. Malinowska, L., Kroschwald, S., and Alberti, S. (2013) Protein disorder, prion propensities, and self-organizing macromolecular collectives. *Biochim. Biophys. Acta* **1834**, 918–931
35. Mitrea, D.M. and Kriwacki, R.W. (2016) Phase separation in biology; functional organization of a higher order. *Cell Commun. Signal.* **14**, 1
36. Masuda, S., Hasegawa, K., Ishii, A., and Ono, T. (2004) Light-induced structural changes in a putative blue-light receptor with a novel FAD binding fold sensor of blue-light using FAD (BLUF); Slr1694 of *Synechocystis* sp. PCC6803. *Biochemistry* **43**, 5304–5313
37. Yuan, H. and Bauer, C.E. (2008) PixE promotes dark oligomerization of the BLUF photoreceptor PixD. *Proc. Natl. Acad. Sci. USA* **105**, 11715–11719
38. Weber, S.C. and Brangwynne, C.P. (2012) Getting RNA and protein in phase. *Cell* **149**, 1188–1191
39. Li, P., Banjade, S., Cheng, H.-C., Kim, S., Chen, B., Guo, L., Llaguno, M., Hollingsworth, J.V., King, D.S., Banani, S.F., Russo, P.S., Jiang, Q.-X., Nixon, B.T., and Rosen, M.K. (2012) Phase transitions in the assembly of multivalent signalling proteins. *Nature* **483**, 336–340
40. Shin, Y., Berry, J., Pannucci, N., Haataja, M.P., Toettcher, J.E., and Brangwynne, C.P. (2017) Spatiotemporal control of intracellular phase transitions using light-activated optoDroplets. *Cell* **168**, 159–171.e14
41. Bugaj, L.J., Choksi, A.T., Mesuda, C.K., Kane, R.S., and Schaffer, D.V. (2013) Optogenetic protein clustering and signaling activation in mammalian cells. *Nat. Methods* **10**, 249–252
42. Dine, E., Gil, A.A., Uribe, G., Brangwynne, C.P., and Toettcher, J.E. (2018) Protein phase separation provides long-term memory of transient spatial stimuli. *Cell Syst.* **6**, 655–663.e5
43. Bracha, D., Walls, M.T., Wei, M.-T., Zhu, L., Kurian, M., Avalos, J.L., Toettcher, J.E., and Brangwynne, C.P. (2018) Mapping local and global liquid phase behavior in living cells using photo-oligomerizable seeds. *Cell* **175**, 1467–1480.e13
44. Guntas, G., Hallett, R.A., Zimmerman, S.P., Williams, T., Yumerefendi, H., Bear, J.E., and Kuhlman, B. (2015) Engineering an improved light-induced dimer (iLID) for

- controlling the localization and activity of signaling proteins. *Proc. Natl. Acad. Sci. USA* **112**, 112–117
45. Shin, Y., Chang, Y.-C., Lee, D.S.W., Berry, J., Sanders, D.W., Ronceray, P., Wingreen, N.S., Haataja, M., and Brangwynne, C.P. (2018) Liquid nuclear condensates mechanically sense and restructure the genome. *Cell* **175**, 1481–1491.e13
  46. Tanenbaum, M.E., Gilbert, L.A., Qi, L.S., Weissman, J.S., and Vale, R.D. (2014) A protein-tagging system for signal amplification in gene expression and fluorescence imaging. *Cell* **159**, 635–646
  47. Navarro, M.G.-J., Kashida, S., Chouaib, R., Souquere, S., Pierron, G., Weil, D., and Gueroui, Z. (2018) RNA is a critical element for the sizing and the composition of phase-separated RNA-protein condensates. *bioRxiv*. 10.1101/457986
  48. Rollins, C.T., Rivera, V.M., Woolfson, D.N., Keenan, T., Hatada, M., Adams, S.E., Andrade, L.J., Yaeger, D., van Schravendijk, M.R., Holt, D.A., Gilman, M., and Clackson, T. (2000) A ligand-reversible dimerization system for controlling protein-protein interactions. *Proc. Natl. Acad. Sci. USA* **97**, 7096–7101
  49. Jain, A. and Vale, R.D. (2017) RNA phase transitions in repeat expansion disorders. *Nature* **546**, 243–247
  50. Watanabe, T., Seki, T., Fukano, T., Sakaue-Sawano, A., Karasawa, S., Kubota, M., Kurokawa, H., Inoue, K., Akatsuka, J., and Miyawaki, A. (2017) Genetic visualization of protein interactions harnessing liquid phase transitions. *Sci. Rep.* **7**, 46380
  51. Schuster, B.S., Reed, E.H., Parthasarathy, R., Jahnke, C.N., Caldwell, R.M., Bermudez, J.G., Ramage, H., Good, M.C., and Hammer, D.A. (2018) Controllable protein phase separation and modular recruitment to form responsive membraneless organelles. *Nat. Commun.* **9**, 2985
  52. Elbaum-Garfinkle, S., Kim, Y., Szczepaniak, K., Chen, C.C.-H., Eckmann, C.R., Myong, S., and Brangwynne, C.P. (2015) The disordered P granule protein LAF-1 drives phase separation into droplets with tunable viscosity and dynamics. *Proc. Natl. Acad. Sci. USA* **112**, 7189–7194
  53. Thompson, K.E., Bashor, C.J., Lim, W.A., and Keating, A.E. (2012) SYNZIP protein interaction toolbox: in vitro and in vivo specifications of heterospecific coiled-coil interaction domains. *ACS Synth. Biol.* **1**, 118–129
  54. Frey, S. and Görlich, D. (2009) FG/FxFG as well as GLFG repeats form a selective permeability barrier with self-healing properties. *EMBO J.* **28**, 2554–2567
  55. Hülsmann, B.B., Labokha, A.A., and Görlich, D. (2012) The permeability of reconstituted nuclear pores provides direct evidence for the selective phase model. *Cell* **150**, 738–751
  56. Kato, M., Han, T.W., Xie, S., Shi, K., Du, X., Wu, L.C., Mirzaei, H., Goldsmith, E.J., Longgood, J., Pei, J., Grishin, N.V., Frantz, D.E., Schneider, J.W., Chen, S., Li, L., Sawaya, M.R., Eisenberg, D., Tycko, R., and McKnight, S.L. (2012) Cell-free formation of RNA granules: low complexity sequence domains form dynamic fibers within hydrogels. *Cell* **149**, 753–767
  57. Han, T.W., Kato, M., Xie, S., Wu, L.C., Mirzaei, H., Pei, J., Chen, M., Xie, Y., Allen, J., Xiao, G., and McKnight, S.L. (2012) Cell-free formation of RNA granules: bound RNAs identify features and components of cellular assemblies. *Cell* **149**, 768–779
  58. Patel, A., Lee, H.O., Jawerth, L., Maharana, S., Jahnke, M., Hein, M.Y., Stoykov, S., Mahamid, J., Saha, S., Franzmann, T.M., Pozniakovski, A., Poser, I., Maghelli, N., Royer, L.A., Weigert, M., Myers, E.W., Grill, S., Drechsel, D., Hyman, A.A., and Alberti, S. (2015) A liquid-to-solid phase transition of the ALS protein FUS accelerated by disease mutation. *Cell* **162**, 1066–1077
  59. Murakami, T., Qamar, S., Lin, J.Q., Schierle, G.S.K., Rees, E., Miyashita, A., Costa, A.R., Dodd, R.B., Chan, F.T.S., Michel, C.H., Kronenberg-Versteeg, D., Li, Y., Yang, S.-P., Wakutani, Y., Meadows, W., Ferry, R.R., Dong, L., Tartaglia, G.G., Favrin, G., Lin, W.-L., Dickson, D.W., Zhen, M., Ron, D., Schmitt-Ulms, G., Fraser, P.E., Shneider, N.A., Holt, C., Vendruscolo, M., Kaminski, C.F., and St George-Hyslop, P. (2015) ALS/FTD mutation-induced phase transition of FUS liquid droplets and reversible hydrogels into irreversible hydrogels impairs RNP granule function. *Neuron* **88**, 678–690
  60. Nakamura, H., Lee, A.A., Afshar, A.S., Watanabe, S., Rho, E., Razavi, S., Suarez, A., Lin, Y.-C., Tanigawa, M., Huang, B., DeRose, R., Bobb, D., Hong, W., Gabelli, S.B., Goutsias, J., and Inoue, T. (2018) Intracellular production of hydrogels and synthetic RNA granules by multivalent molecular interactions. *Nat. Mater.* **17**, 79–89
  61. Xiang, S., Kato, M., Wu, L.C., Lin, Y., Ding, M., Zhang, Y., Yu, Y., and McKnight, S.L. (2015) The LC domain of hnRNPA2 adopts similar conformations in hydrogel polymers, liquid-like droplets, and nuclei. *Cell* **163**, 829–839
  62. Yang, Z.M., Xu, K.M., Guo, Z.F., Guo, Z.H., and Xu, B. (2007) Intracellular enzymatic formation of nanofibers results in hydrogelation and regulated cell death. *Adv. Mater.* **19**, 3152–3156
  63. Dubnikov, T., Ben-Gedalya, T., and Cohen, E. (2017) Protein quality control in health and disease. *Cold Spring Harb. Perspect. Biol.* **9**, a023523
  64. Eisenberg, D. and Jucker, M. (2012) The amyloid state of proteins in human diseases. *Cell* **148**, 1188–1203
  65. West, M.W., Wang, W., Patterson, J., Mancias, J.D., Beasley, J.R., and Hecht, M.H. (1999) De novo amyloid proteins from designed combinatorial libraries. *Proc. Natl. Acad. Sci. USA* **96**, 11211–11216
  66. Olzscha, H., Schermann, S.M., Woerner, A.C., Pinkert, S., Hecht, M.H., Tartaglia, G.G., Vendruscolo, M., Hayer-Hartl, M., Hartl, F.U., and Vabulas, R.M. (2011) Amyloid-like aggregates sequester numerous metastable proteins with essential cellular functions. *Cell* **144**, 67–78
  67. Zhang, K., Donnelly, C.J., Haeusler, A.R., Grima, J.C., Machamer, J.B., Steinwald, P., Daley, E.L., Miller, S.J., Cunningham, K.M., Vidensky, S., Gupta, S., Thomas, M.A., Hong, I., Chiu, S.-L., Haganir, R.L., Ostrow, L.W., Matunis, M.J., Wang, J., Sattler, R., Lloyd, T.E., and Rothstein, J.D. (2015) The C9orf72 repeat expansion disrupts nucleocytoplasmic transport. *Nature* **525**, 56–61
  68. Freibaum, B.D., Lu, Y., Lopez-Gonzalez, R., Kim, N.C., Almeida, S., Lee, K.-H., Badders, N., Valentine, M., Miller, B.L., Wong, P.C., Petrucelli, L., Kim, H.J., Gao, F.-B., and Taylor, J.P. (2015) GGGGCC repeat expansion in C9orf72 compromises nucleocytoplasmic transport. *Nature* **525**, 129–133
  69. Woerner, A.C., Frottin, F., Hornburg, D., Feng, L.R., Meissner, F., Patra, M., Tatzelt, J., Mann, M., Winklhofer, K.F., Hartl, F.U., and Hipp, M.S. (2016) Cytoplasmic protein aggregates interfere with

- nucleocytoplasmic transport of protein and RNA. *Science* **351**, 173–176
70. Miyazaki, Y., Mizumoto, K., Dey, G., Kudo, T., Perrino, J., Chen, L.-C., Meyer, T., and Wandless, T.J. (2016) A method to rapidly create protein aggregates in living cells. *Nat. Commun.* **7**, 11689
  71. He, R.-Y., Chao, S.-H., Tsai, Y.-J., Lee, C.-C., Yu, C.-Y., Gao, H.-D., Huang, Y.-A., Hwang, E., Lee, H.-M., and Huang, J.J.-T. (2017) Photocontrollable probe spatiotemporally induces neurotoxic fibrillar aggregates and impairs nucleocytoplasmic trafficking. *ACS Nano* **11**, 6795–6807
  72. Tsutsui, H., Jinno, Y., Shoda, K., Tomita, A., Matsuda, M., Yamashita, E., Katayama, H., Nakagawa, A., and Miyawaki, A. (2015) A diffraction-quality protein crystal processed as an autophagic cargo. *Mol. Cell* **58**, 186–193
  73. Tsutsui, H., Karasawa, S., Shimizu, H., Nukina, N., and Miyawaki, A. (2005) Semi-rational engineering of a coral fluorescent protein into an efficient highlighter. *EMBO Rep.* **6**, 233–238
  74. Lee, S., Lee, K.H., Ha, J.-S., Lee, S.-G., and Kim, T.K. (2011) Small-molecule-based nanoassemblies as inducible nanoprobe for monitoring dynamic molecular interactions inside live cells. *Angew. Chem. Int. Ed.* **50**, 8709–8713
  75. Taslimi, A., Vrana, J.D., Chen, D., Borinskaya, S., Mayer, B.J., Kennedy, M.J., and Tucker, C.L. (2014) An optimized optogenetic clustering tool for probing protein interaction and function. *Nat. Commun.* **5**, 4925
  76. Park, H., Kim, N.Y., Lee, S., Kim, N., Kim, J., and Heo, W.D. (2017) Optogenetic protein clustering through fluorescent protein tagging and extension of CRY2. *Nat. Commun.* **8**, 30
  77. Stoecklin, G. and Kedersha, N. (2013) Relationship of GW/P-bodies with stress granules in *Ten Years of Progress in GW/P Body Research* (Chan, E. K. L. and Fritzler, M. J. eds.) pp. 197–211, Advances in Experimental Medicine and Biology, Springer, NY
  78. Wan, G., Fields, B.D., Spracklin, G., Shukla, A., Phillips, C.M., and Kennedy, S. (2018) Spatiotemporal regulation of liquid-like condensates in epigenetic inheritance. *Nature* **557**, 679–683
  79. Vance, C., Scotter, E.L., Nishimura, A.L., Troakes, C., Mitchell, J.C., Kathe, C., Urwin, H., Manser, C., Miller, C.C., Hortobágyi, T., Dragunow, M., Rogelj, B., and Shaw, C.E. (2013) ALS mutant FUS disrupts nuclear localization and sequesters wild-type FUS within cytoplasmic stress granules. *Hum. Mol. Genet.* **22**, 2676–2688
  80. Baron, D.M., Kaushansky, L.J., Ward, C.L., Sama, R.R.K., Chian, R.-J., Boggio, K.J., Quaresma, A.J.C., Nickerson, J.A., and Bosco, D.A. (2013) Amyotrophic lateral sclerosis-linked FUS/TLS alters stress granule assembly and dynamics. *Mol. Neurodegener.* **8**, 30
  81. Boeynaems, S., Bogaert, E., Kovacs, D., Konijnenberg, A., Timmerman, E., Volkov, A., Guharoy, M., De Decker, M., Jaspers, T., Ryan, V.H., Janke, A.M., Baatsen, P., Vercruyse, T., Kolaitis, R.-M., Daelemans, D., Taylor, J.P., Kedersha, N., Anderson, P., Impens, F., Sobott, F., Schymkowitz, J., Rousseau, F., Fawzi, N.L., Robberecht, W., Van Damme, P., Tompa, P., and Van Den Bosch, L. (2017) Phase separation of C9orf72 dipeptide repeats perturbs stress granule dynamics. *Mol. Cell* **65**, 1044–1055.e5
  82. Zhang, K., Daigle, J.G., Cunningham, K.M., Coyne, A.N., Ruan, K., Grima, J.C., Bowen, K.E., Wadhwa, H., Yang, P., Rigo, F., Taylor, J.P., Gitler, A.D., Rothstein, J.D., and Lloyd, T.E. (2018) Stress granule assembly disrupts nucleocytoplasmic transport. *Cell* **173**, 958–971.e17
  83. Guo, L. and Shorter, J. (2015) It's raining liquids: RNA tunes viscoelasticity and dynamics of membraneless organelles. *Mol. Cell* **60**, 189–192
  84. Langdon, E.M., Qiu, Y., Ghanbari Niaki, A., McLaughlin, G.A., Weidmann, C.A., Gerbich, T.M., Smith, J.A., Crutchley, J.M., Termini, C.M., Weeks, K.M., Myong, S., and Gladfelter, A.S. (2018) mRNA structure determines specificity of a polyQ-driven phase separation. *Science* **360**, 922–927
  85. Van Treeck, B. and Parker, R. (2018) Emerging roles for intermolecular RNA-RNA interactions in RNP assemblies. *Cell* **174**, 791–802
  86. Boke, E., Ruer, M., Wühr, M., Coughlin, M., Lemaitre, R., Gygi, S.P., Alberti, S., Drechsel, D., Hyman, A.A., and Mitchison, T.J. (2016) Amyloid-like self-assembly of a cellular compartment. *Cell* **166**, 637–650
  87. Berchowitz, L.E., Kabachinski, G., Walker, M.R., Carlile, T.M., Gilbert, W.V., Schwartz, T.U., and Amon, A. (2015) Regulated formation of an amyloid-like translational repressor governs gametogenesis. *Cell* **163**, 406–418
  88. Feric, M., Vaidya, N., Harmon, T.S., Mitrea, D.M., Zhu, L., Richardson, T.M., Kriwacki, R.W., Pappu, R.V., and Brangwynne, C.P. (2016) coexisting liquid phases underlie nucleolar subcompartments. *Cell* **165**, 1686–1697
  89. Gallo, C.M., Wang, J.T., Motegi, F., and Seydoux, G. (2010) Cytoplasmic partitioning of P granule components is not required to specify the germline in *C. elegans*. *Science* **330**, 1685–1689
  90. Anderson, P. and Kedersha, N. (2002) Stressful initiations. *J. Cell Sci.* **115**, 3227–3234
  91. Liu-Yesucevitz, L., Bilgutay, A., Zhang, Y.-J., Vanderweyde, T., Vanderwyde, T., Citro, A., Mehta, T., Zaarur, N., McKee, A., Bowser, R., Sherman, M., Petrucelli, L., and Wolozin, B. (2010) Tar DNA binding protein-43 (TDP-43) associates with stress granules: analysis of cultured cells and pathological brain tissue. *PLoS One* **5**, e13250